Appl Phys A
DOI 10.1007/s00339-013-7907-9

Applied Physics A
Materials Science & Processing

INVITED PAPER

Fabrication of a bulk silicon p–n homojunction-structured light-emitting diode showing visible electroluminescence at room temperature

Minh Anh Tran · Tadashi Kawazoe · Motoichi Ohtsu

Received: 31 July 2013 / Accepted: 1 August 2013

Abstract We have developed a novel dressed-photon-assisted annealing process, in which the distribution of dopant (boron) domains is modified in a self-organized manner based on the absorption of light having a photon energy higher than the band gap and subsequent stimulated emission. Using this process, we were able to fabricate a bulk silicon p–n homojunction-structured light-emitting diode that showed electroluminescence emission in the visible region at room temperature. A broadband spectrum with three emission peaks at 400 nm, 590 nm, and 620 nm was clearly observed.

1 Introduction

The possibility of achieving light emission from silicon (Si) has been receiving much attention for many years because of the numerous advantages of Si. One major advantage is the ability to produce high-quality Si from silica, the second most abundant material in the surface of the Earth, using a well-developed conventional electric arc furnace process without any toxic emissions [1]. Thus, Si light-emitting diodes (LEDs) have a greater ease of processing and lower cost and will be more environmentally friendly than conventional LEDs made from exotic and often toxic chemical compounds, e.g., InGaAsP. However, because Si is an indirect band gap material, electrons and holes cannot recombine easily due to the momentum conservation law; this results in an extremely low efficiency of spontaneous emission in silicon [2]. Despite the many efforts, over decades, that researchers have been making to achieve light emission from Si, there still remains a significant demand for an efficient solution that can address the so-called "indirect band gap dilemma" [3].

One promising method for achieving light emission from Si is to generate dressed photons (DPs) by forming a suitable dopant density distribution inside a Si crystal [4]. A DP is a quasi-particle representing the coupled state of a photon and an electron–hole pair. It has been found that the DP excites a multi-mode coherent phonon, forming a quasi-particle representing the coupled state of a DP and a multi-mode coherent phonon, called a dressed-photon–phonon (DPP) [5]. A DPP can efficiently provide the necessary momentum for the radiative recombination of the electron–hole pair. In recent research by the authors, we succeeded in fabricating such a structure in Si by employing a technique known as DP-assisted annealing, which allowed us to realize a high-efficiency p–n homojunction-structured LED using a bulk Si crystal [4]. This annealing process has also been applied not only to a Si infrared LED but also to a Si infrared laser [6], a Si photodetector [7], a Si optical and electrical relaxation oscillator [8], and a ZnO LED [9]. However, the light emitted from the devices fabricated using this annealing principle resulted from a two-step transition of an electron in the conduction band to the valence band; hence, the photon energy of the light cannot exceed the band gap energy of the material. For example, the Si LED fabricated by using this annealing method could only emit light in the infrared region (0.75–0.95 eV) [4], which is lower than the Si band gap energy ($E_g = 1.12$ eV).

The purpose of this study was to develop a new annealing technique that can transcend the above limitation. We describe the principle of a new DP-assisted annealing method that enables the emission of light with a photon energy higher than the band gap energy. Instead of using

M.A. Tran · T. Kawazoe (✉) · M. Ohtsu
Graduate School of Engineering, The University of Tokyo,
2-11-16 Yayoi, Bunkyo-ku, Tokyo 113-8656, Japan
e-mail: kawazoe@ee.t.u-tokyo.ac.jp

Published online: 14 August 2013

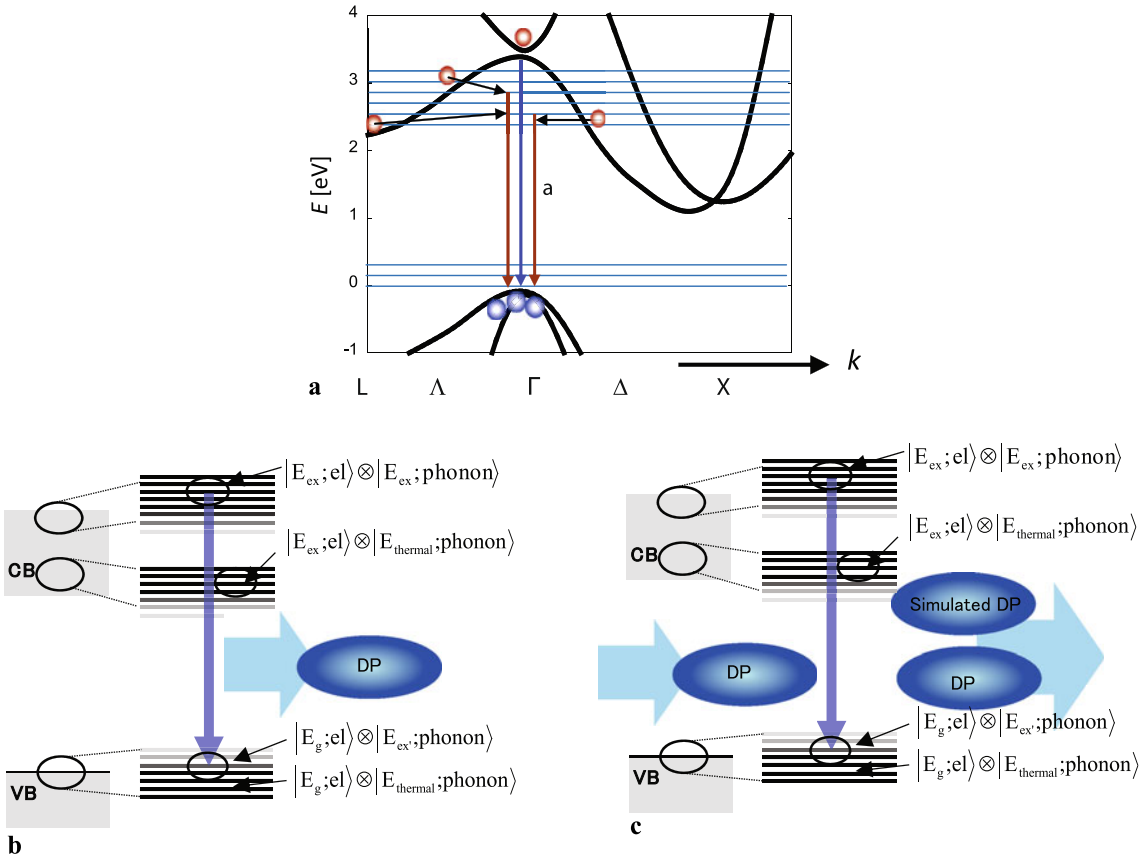

Fig. 1 (**a**) Schematic diagram of the radiative relaxation of an electron from a high-energy excited state via a DPP-assisted process. *Blue horizontal blue lines* represent the phonon-coupled electronic states. (**b**), (**c**) DPP models for energy transitions via DPP-assisted process in radiative relaxation of high-excited state electron from high energy level. The *vertical arrows* represent the relaxation process of electron. (**b**) shows the spontaneous emission process when a DP is emitted. (**c**) shows the stimulated emission process when a DP stimulates the emission of one more identical DP

a two-step transition as in the previous research, the photon is emitted in a relaxation transition of the electron from its excited high-energy state; hence, the photon energy of the emitted light can be higher than the band gap energy of the material. By applying this new DP-assisted annealing technique, we successfully fabricated a Si bulk p–n homojunction-structured LED that emitted light in the visible region (whose photon energy is two times higher than the band gap energy of Si) at room temperature. The principle of light emission, the annealing technique, the fabrication process, and characteristics of the Si visible LED are described in detail.

2 Principle of light emission with photon energy higher than band gap

In this section, we explain the operating principle of our Si visible LED. The fabrication will be described later because the operating principle will also be used in the fabrication process. As was pointed out in the previous section, a DPP can provide a certain momentum for the recombination of an electron and hole because the phonon in the DPP is a multimode phonon. This characteristic was used in our previous research to accomplish infrared light emission from a bulk Si crystal [4, 6, 8]. Although the lowest point of the conduction band (X-point) and the highest point of the valence band (Γ-point) correspond to different momenta, an electron in the conduction band efficiently relaxes to the ground state and emits a photon thanks to the assistance of the phonon in the DPP. Furthermore, radiative transition from a high-energy excited electron can also easily occur via the DPP (Fig. 1(a)). For example, due to the existence of the DPP at a high energy (e.g., level *a* in Fig. 1(a)), an excited-state electron nearby can quickly couple with the coherent phonon and then directly relax to the ground state; thus, a radiative relaxation shown by the red arrow occurs and results in emission with a photon energy higher than the band gap energy. Recall that, without the DP, an electron in an excited state at high energy quickly transitions to the lowest point in the conduction band due to fast intra-band relaxation; there-

fore, the probability of a transition from a high-energy excited state is extremely low in conventional methods.

In the DPP model shown in Fig. 1(b) and (c), since the electron–hole pair strongly couples with the photon and phonon, the energy state is expressed as the direct product of the ket vectors of the electronic state and the phonon state. For example, $|E_g; el\rangle \otimes |E_{thermal}; phonon\rangle$ includes the ground state of the electron and the thermal equilibrium state of the phonon. The spontaneous emission of a DP (Fig. 1(b)) is the result of the radiative transition from the initial state $|E_{ex}; el\rangle \otimes |E_{ex}; phonon\rangle$ to the ground state $|E_g; el\rangle \otimes |E_{ex'}; phonon\rangle$. After the transition, the phonon excited state relaxes to the thermal equilibrium state determined by the crystal lattice temperature and ends with a transition to the electronic ground state $|E_g; el\rangle \otimes |E_{thermal}; phonon\rangle$. In addition, the stimulated emission process (Fig. 1(c)) is explained as follows. When an electron in the conduction band is irradiated with a DP, the electron transitions from the initial state $|E_{ex}; el\rangle \otimes |E_{ex}; phonon\rangle$ to the ground state $|E_g; el\rangle \otimes |E_{ex'}; phonon\rangle$, and emits light. When the electron number densities of occupation in the initial state $|E_{ex}; el\rangle \otimes |E_{ex}; phonon\rangle$ and the intermediate state $|E_g; el\rangle \otimes |E_{ex'}; phonon\rangle$, denoted by n_{ex} and n_g, satisfy the Bernard–Duraffourg inversion condition ($n_{ex} > n_g$) [10], the number of photons created by stimulated emission exceeds the number of photons annihilated by absorption. Like spontaneous emission, the phonon then relaxes to a thermal equilibrium state determined by the crystal lattice temperature, and ends with a transition to the electronic ground state $|E_g; el\rangle \otimes |E_{thermal}; phonon\rangle$.

In order to realize a Si p–n homojunction-structured LED that emits light in the visible region, the two emission processes described above were used two times. The first was for fabrication of the device, more specifically, for the self-organization of the spatial distribution of the dopant suitable for the emission of high-energy photons. The second was for the operation of the device, to obtain spontaneously emitted light with a photon energy higher than the band gap energy. These are described in the following sections.

3 Dressed-photon-assisted annealing process

In order to form a suitable nanostructure for generating DPPs to assist the radiative transition of electrons from a high energy level, we used a DP-assisted annealing technique. As a preparation before annealing, a dopant (boron: B) is implanted into a low-electrical-resistivity n-type wafer, forming a p-layer with an inhomogeneous dopant distribution. Then, the annealing process is carried out by applying a forward bias voltage to the crystal while irradiating it with a laser beam from the p-layer side. The laser light has a photon energy E_{anneal} which is higher than the band gap energy E_g ($E_{anneal} > E_g$), and the forward bias voltage is set to be higher than E_{anneal}/e, where e represents the electron charge. During this annealing process, the dopant distribution at the p–n junction is continuously modified in a self-organized manner until reaching the desirable shape via the following mechanisms.

(1) At dopant domains where DPPs are hardly generated: The incoming photon excites an electron from the ground state in the valence band to an excited state in the conduction band. The non-absorbed excess energy, $E_{anneal} - E_g$, is quickly converted to thermal energy via fast intra-band relaxation of electrons. Moreover, because of the indirect band gap, the electron will relax to the ground state via a non-radiative process, and the energy of the electron is converted to thermal energy. Thus, as a whole, the optical energy of the laser beam is converted to the heat in crystal. It is this heat that causes the dopant to diffuse; as a result, the spatial distribution of the dopant domains changes.
(2) At the dopant domains where DPPs are easily generated: Since electrons having energy higher than E_{anneal} are injected sufficiently by the forward bias current to satisfy the Bernard–Duraffourg inversion condition, stimulated emission via the DPPs is triggered. Due to this stimulated emission, the energy of the laser beam is converted to optical energy, instead of heat, as in the domains where DPPs are not generated. Thus, it becomes more difficult to bring about heat-induced changes in the dopant distribution.

At the domains where stimulated emission via DPPs strongly occurs, the shape and dimension of the inhomogeneous dopant distribution become stable, whereas at the other domains where the conditions are unsuitable for DPP generation, the dopant distribution keeps changing due to the annealing heat. Furthermore, since the probability of spontaneous emission is proportional to that of stimulated emission, spontaneous emission via DPPs also tends to occur in regions where stimulated emission tends to occur. Therefore, as the annealing advances, together with temporal evolution of the dopant distribution, the stimulated emitted light spreads through the whole device. After a sufficient DP assisted annealing, all of the dopant domains reach a stable profile, in which the probability of stimulated emission via DPPs becomes significantly high. It can be expected that the spatial distribution of the dopant formed after this annealing process will be optimized for the spontaneous emission of light having high photon energy.

4 Device fabrication

The fabrication of the device can be divided into two steps. The first step is to prepare a Si p–n homojunction structure

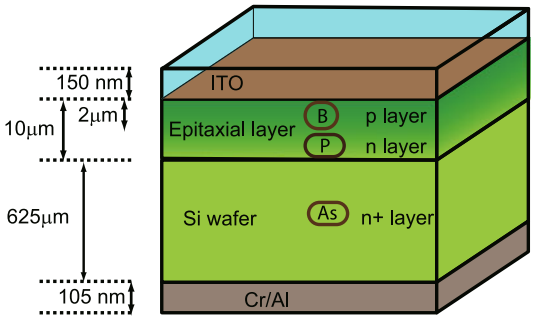

Fig. 2 Structure of Si LED with a p–n homojunction

having a modifiable dopant distribution. The second step is to modify the shape of the dopant domains through the DP-assisted annealing process described above.

In the first step, we used an As-doped n-type Si single crystal on which we deposited an epitaxial layer of phosphorus (P). This Si crystal was doped with boron (B) by an ion implantation method, with seven different levels of accelerating energy of 30, 70, 130, 215, 330, 480, and 700 keV, to form dopant domains with a dose density of 10^{19} cm^{-3}. A p-type region was successfully formed in Si, and as a result, a p–n homojunction structure was constructed. Furthermore, with such a high energy and high-concentration B-doping profile, the distribution of B at the p–n junction was spatially inhomogeneous; this was to increase the probability of producing a dopant distribution favorable for generating DPs. The crystal was then diced into a 5 mm × 5 mm area. A 150 nm-thick indium tin oxide (ITO) film was deposited on the surface of the p-type layer, whereas a 5 nm-thick Cr film and a 100 nm-thick Al film were deposited on the back surface of the n-type Si to serve as electrodes, by using RF sputtering. The layer structure of the device is shown in Fig. 2.

In the second step, the DP-assisted annealing was performed by causing a forward bias current to flow through the device while irradiating the p-type side of the device with a laser beam. The experimental setup is illustrated in Fig. 3. To connect the electric power supply to the device, Dotite paste was used to attach a Cu film on the p-type surface. Another Cu film was also attached to the n-type side of the device. The forward bias current density used for the annealing was 1.44 A/cm^2, and the optical power of the laser beam irradiation was 75 mW. At the surface of the device, the laser beam radius was 1.5 mm, and so the irradiation light density was approximately 3.33 W/cm^2, which is high enough for inducing the DP-assisted annealing. The wavelength of the laser light was 400 nm; in other words, the photon energy was 3.1 eV, which is 2.5 times higher than the band gap energy of Si. After one hour of annealing, the fabrication of our Si homojunction-structured LED was completed.

To confirm the stimulated emission, Fig. 4 shows the results of measuring the change in surface temperature difference between the irradiated area and the non-irradiated area. The Si crystal was continuously irradiated with light, and current injection was started after 7 minutes. At the beginning, when only the laser beam was radiated, the temperature difference dramatically increased due to the heat generated by light absorption. After a few minutes, the heat gradually diffused into the whole device, and the temperature difference reached a stable state. This agreed with our hypothesis of how the annealing process advances with laser irradiation, which was described in (1) and (2) in the previous section. Next, after 7 minutes, a forward bias voltage was applied to the device, while continuing to radiate the laser beam. This led to an obvious decrease in the temperature difference. This decrease was a result of stimulated emission in the area where DPs were generated: The irradiation light was not converted into heat, but induced light emission due to the stimulated emission process. In other words, the decrease in temperature difference when an electrical bias was applied has confirmed the occurrence of stimulated emission of DPPs.

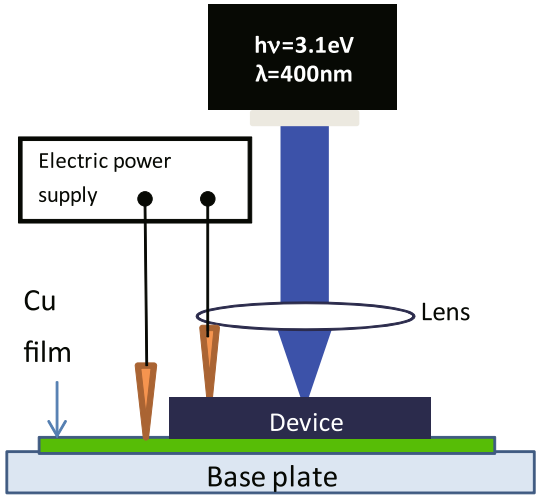

Fig. 3 Experimental setup for dressed-photon-assisted annealing process

5 Device characterization

In this section, we present the electroluminescence (EL) characteristics and electrical characteristics of the fabricated device. We also discuss the physical mechanism of the device operation.

5.1 Electroluminescence spectrum at room temperature

Figure 5 shows photographs of the external appearance of the non-biased and forward-biased (voltage 7 V, current density 2 A/cm^2) device taken with a band-filtered visible CCD

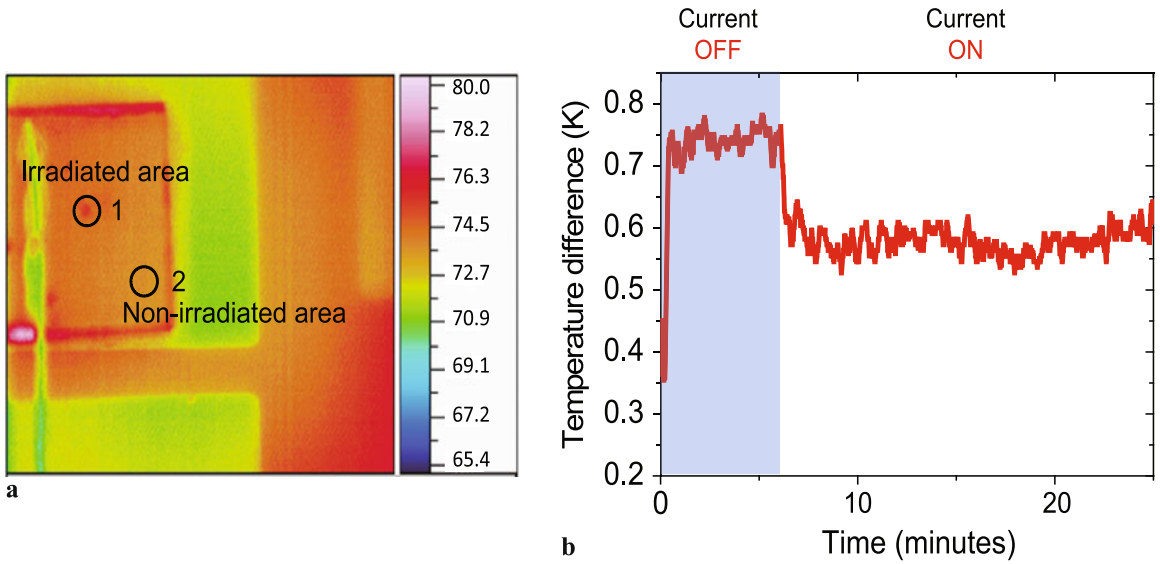

Fig. 4 Surface temperature variation due to DPP stimulated emission. (**a**) Thermography image of the device surface temperature. (**b**) The vertical axis shows the temperature difference between an area irradiated by the laser beam (*area 1*) and a non-irradiated area (*area 2*). The device was continuously irradiated with laser, while current was injected only after seventh minute

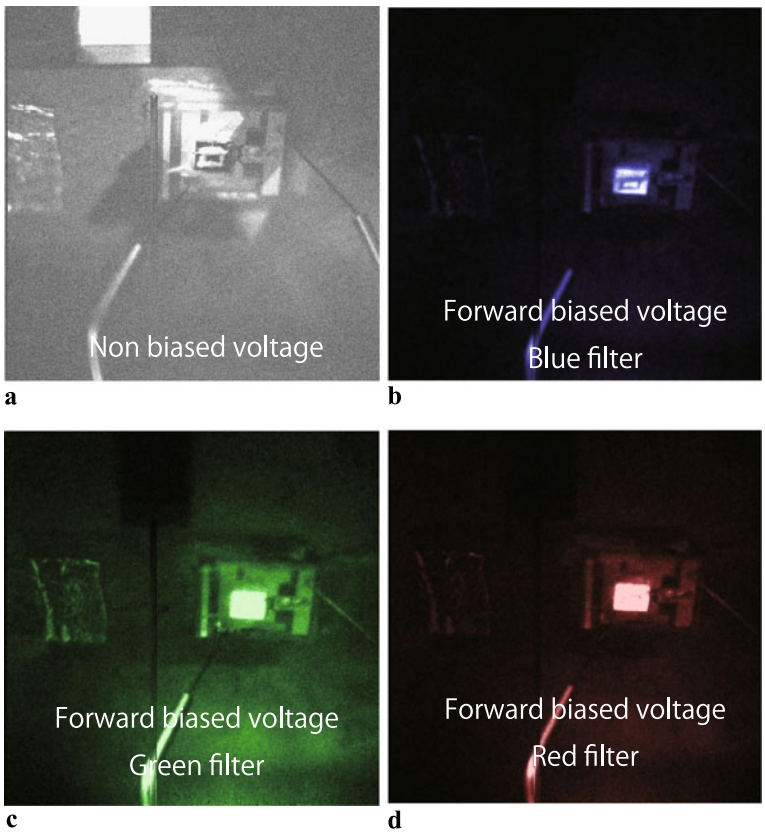

Fig. 5 Photographs of device emitting light at room temperature, captured with a CCD camera. (**a**) No forward-bias voltage. (**b**), (**c**), (**d**) A forward-bias voltage of 4.5 V was applied. Blue, green, and red band pass filters (center wavelengths of 450 nm, 550 nm, and 650 nm, respectively) were used

camera at room temperature. Figure 5(b)–(d) clearly reveal that the light emission spectrum from our Si LED contained all three primary colors: blue, green, and red. This confirms that the fabricated Si LED showed EL emission in the visible region when a forward-bias voltage was applied.

We studied the EL spectrum of the Si LED when a forward-bias voltage was applied. The curves in Fig. 6 are visible-region EL spectra of our device at room temperature before and after the DP-assisted annealing process. As we can see, no EL emission was observed before the anneal-

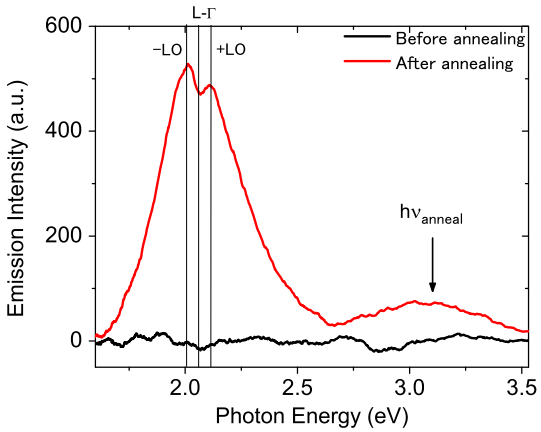

Fig. 6 EL spectra of the Si LED. *Black* and *red curves* show emission before and after the dressed-photon-assisted annealing, respectively. The *vertical lines* (shown as −LO, L-Γ and +LO) represent specific values of $E_{L-\Gamma} - E_{1\text{ LO phonon}}$, $E_{L-\Gamma}$, and $E_{L-\Gamma} + E_{1\text{ LO phonon}}$ respectively

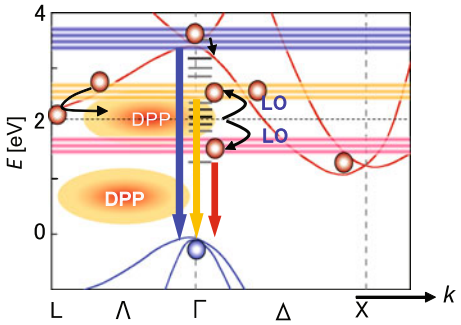

Fig. 7 Schematic diagram of light emission in visible region from Si. *Red* and *blue curves* represent the energy levels of the conduction and valence bands. *Blue*, *orange*, and *gray thick horizontal lines* represent the phonon levels corresponding to 3.1 eV, 2.1 eV, and 2.0 eV, respectively. Via phonon levels, electrons in high-energy excited states at the Γ-point and L-point of the conduction band can radiatively relax to the ground state with a high probability. Interactions with longitudinal optical phonons (LO) result in two split energy levels from which excited electrons at the L-point of the conduction band transition to the ground state

ing. After the annealing, a broad EL spectrum appeared. Noticeably, there exist three dominant peaks in the EL spectra: the first one at 3.1 eV (wavelength 400 nm), which corresponds to blue, and the other two close peaks at photon energies 2.0 eV (wavelength 620 nm) and 2.1 eV (wavelength 590 nm), which correspond to red and green.

The above EL emission characteristics of our Si LED agree with the light emission principle we proposed in Sect. 2 and will be explained in detail here. Figure 7 shows the band structure of Si (red and blue curves) and the phonon-coupled electronic levels (in particular, the blue, orange, and gray thick horizontal lines represent phonon levels involved in the light emission in the visible region). Since a DP strongly couples with phonons, a transition between the phonon-coupled electronic levels appears if the probability of a DP that is resonant with the transition energy is high. After the annealing process, almost all the B domains in Si become suitable for generating DPs whose photon energy corresponds to the light radiated during annealing. Because the photon energy of the annealing light was 3.1 eV ($\lambda = 400$ nm), high-energy excited electrons at the Γ-point of the conduction band likely relaxed to the ground state via those 3.1 eV photon levels, resulting in the spectral peak at 3.1 eV in the EL spectrum. Moreover, the injected electrons also tend to relax to the lower energy level via intra-band relaxation, i.e., the L- and X-points in the conduction band. Therefore, the density of electrons at those points in the conduction band is considerably high. Because the emission intensity is also proportional to the number of electrons, the radiative transition of electrons from the L-point results in light emission in the proximity of 2.0 eV.

The broad spectrum of the observed EL emission resulted from the interaction of electrons with phonons. Since the probability of phonon interaction is inversely proportional to the number of phonons involved (phonon absorption or emission), the EL spectrum is symmetric with respect to the peak emission values at energies of 2.0 eV, 2.1 eV, and 3.1 eV. Furthermore, the existence of the two peaks in Fig. 6 with photon energies close to the energy level of the L-point indicates the interaction with one longitudinal optical (LO) phonon in the light emission process. The radiative relaxation process of electrons from the L-point to the ground state is also illustrated in Fig. 7. Since there is a large difference in momentum between an electron at the L-point of the conduction band and a hole at the Γ-point of the valence band, according to the momentum conservation law, in order to emit a photon, the electron at the L-point needs to interact with a phonon to lose the excess momentum (or to gain momentum in the case of insufficient momentum). As a result, photons are emitted from two separated energy levels. This explains the existence of two peaks in the vicinity of the L-point, at 2.0 eV and 2.1 eV, as we observed in the EL spectrum in Fig. 6. The energy difference between the two peaks is 100 meV, approximately equivalent to twice the LO phonon energy [11]. The dip between the two peaks corresponds to the zero-phonon line. On the other hand, no similar peaks appear in the spectrum at 3.1 eV. This is because the electrons with an energy of 3.1 eV nearly directly relaxed to the valence band, and thus, the interactions with phonons were weaker.

5.2 Voltage dependence of EL emission intensity

As discussed above, the visible EL emission resulted from the high-energy excited electrons, which are provided by the electrical power source when operating the device as an LED. Therefore, it is necessary to study the dependence of

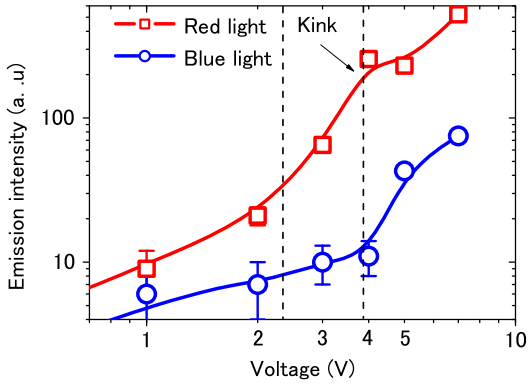

Fig. 8 Relation between the forward-bias voltage and the light emission intensity. *Blue* and *red curves* represent the heights of the peaks in the EL spectrum at 3.1 eV and 2.0 eV in Fig. 6

EL emission performance of the LED on the forward bias voltage. We investigated the dependence of the height of the peak at 3.1 eV (blue light) and the peak at 2.0 eV (red light) in Fig. 6 on the applied voltage. The results are represented by the blue and red curves in Fig. 8. The peak at 2.1 eV (green light) showed behavior similar to the peak at 2.0 eV and is therefore omitted here.

Figure 8 shows that, at a voltage of 2.5 V, the red curve started rising with a higher slope. This corresponds to the threshold for red light emission. Furthermore, at a voltage of about 4 V, the blue curve changed its slope. This kink corresponds to the start of blue light emission. Interestingly, a kink in the red curve is also observed at the kink in the blue curve. This characteristic relation between emission intensity and voltage is well explained by the emission mechanism we discussed above. Assume that the voltage loss due to the Schottky barrier and parasitic circuit resistance is about 1 V. Therefore, when a voltage of 3 V is applied, the highest energy of injected electrons is about 2 eV. Thus, the number density of electrons that have relaxed to the L-point in the conduction band (energy level of about 2 eV) starts rising; therefore, the emission with photon energies of 2.0 and 2.1 eV appears. This transition corresponds to the change in slope of the red curve in Fig. 8. When a sufficiently high forward bias is applied, the energy of injected electrons becomes larger than 3.1 eV, and the density of electrons at the Γ-point increases, resulting in the appearance of emission from a transition with a photon energy corresponding to blue light. This threshold voltage corresponds to the kink in the slope of the blue curve. Here, the appearance of a kink in the red curve is evidence for the fact that some of the injected electrons recombine for the blue light emission, and so the density of electrons that have relaxed to the L-point becomes relatively lower and results in the decreased emission intensity of the red light.

6 Summary

We succeeded in fabricating a light-emitting diode having a p–n homojunction structure by applying a novel dressed-photon-assisted annealing process to an n-type P epitaxial layer on an n-type Si crystal doped with As. The p-type layer was formed by doping B. The device showed a broad EL spectrum in the visible region at room temperature when a forward bias voltage was applied. The emission peak wavelengths of the fabricated device were 400 nm, 590 nm, and 620 nm (photon energies of 3.1 eV, 2.1 eV, and 2.0 eV, respectively). The EL emission and voltage dependence characteristics of the device confirmed that the probability of a radiative relaxation process of electrons from a high-energy excited state was significantly increased due to the assistance of DPPs generated in the Si crystal. This is the world's first demonstration of a bulk Si p–n homojunction-structured LED that shows EL emission in the visible region.

References

1. A. Schei, J.Kr. Tuset, H. Tveit, *Production of High Silicon Alloys* (Tapir Forlag, Trondheim, 1997)
2. D. Liang, J.E. Bowers, Nat. Photonics **4**, 511 (2010)
3. European Commission, *Technology Roadmap: Optoelectronics Interconnects for Integrated Circuits* (Office for Official Publications of the European Communities, Luxembourg, 1998)
4. T. Kawazoe, M. Mueed, M. Ohtsu, Appl. Phys. B **104**, 747 (2011)
5. Y. Tanaka, K. Kobayashi, J. Microsc. **229**, 228 (2008)
6. T. Kawazoe, M. Ohtsu, K. Akahane, N. Yamamoto, Appl. Phys. B **107**, 659 (2012)
7. H. Tanaka, T. Kawazoe, M. Ohtsu, Appl. Phys. B **108**, 51 (2012)
8. N. Wada, T. Kawazoe, M. Ohtsu, Appl. Phys. B **108**, 25 (2012)
9. K. Kitamura, T. Kawazoe, M. Ohtsu, Appl. Phys. B **107**, 637 (2012)
10. M.G.A. Bernald, G. Duraffourg, Phys. Status Solidi **1**, 699 (1961)
11. W. Goldammer, W. Ludwig, W. Zierau, Phys. Rev. B **36**, 4624 (1987)